Chapter 2
Bremsstrahlung in Collisions of Structureless Charged Particles with Atoms and Ions

2.1 Peculiar Features of PBrS

In this section we discuss the peculiar features of PBrS which distinguish this mechanism from OBrS and which strongly influence the total emission spectrum. Focusing on the physical nature of these phenomena and to avoid unnecessary complexities, we consider the BrS process of a non-relativistic charged structureless particle with mass m and charge Z_0 on a spherically-symmetric many-electron target (called an atom, for brevity) within the framework of the simplest approximations, which are (a) the plane-wave first Born approximation for the scattering process, and (b) the dipole-photon scheme for the description of the photon-atom and photon-projectile coupling. Such treatment, although quite often being insufficient for the quantitative description of the process, allows one to carry out a simple qualitative analysis and to explain all specific features of PBrS.

Let $\mathbf{p}_j$ and $\varepsilon_j = p_j^2/2m$ denote the momenta and energy of initial ($j = 1$) and final ($j = 2$) states of the projectile. The initial and the final states of the target atom are assumed to be the ground one. To simplify the formalism we consider the BrS process in the collision with a spherically symmetric neutral atom. This restriction is rather of a formal but not of a principal nature, since the effects described below also occur in the BrS process on a target with a ground state of an arbitrary symmetry.

In the course of the collision, a photon can be emitted via one of the two mechanisms, which are schematically described by Fig. 1.1. The diagrammatic representation of the BrS amplitude is presented in Fig. 2.1 [14]. The thin solid line stands for the projectile, the wave functions of which are described by plane waves $\exp\left(\mathrm{i}\mathbf{p}_j \cdot \mathbf{r}\right)$. The long-dashed line corresponds to the emitted photon which is characterized by the energy ω and the unit vector of polarization $\mathbf{e}$. In the upper two diagrams, which illustrate the OBrS process, the short-dashed vertical line depicts the interaction of the projectile with the atomic static field. The lower diagrams describe the PBrS process in which the Coulomb interaction between the projectile and atomic electrons (vertical dashed line) leads to the virtual excitation $0 \to n$ of the atom.

A. V. Korol and A. V. Solov'yov, *Polarization Bremsstrahlung*,
Springer Series on Atomic, Optical, and Plasma Physics 80,
DOI: 10.1007/978-3-642-45224-6_2, © Springer-Verlag Berlin Heidelberg 2014

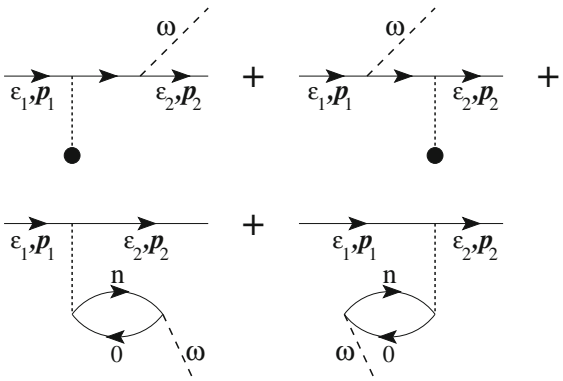

Fig. 2.1 Diagrammatic representation of the amplitude of BrS of a fast electron on an atom in the Born approximation. *Two upper* diagrams describe ordinary BrS, *two lower* ones—polarizational BrS

Considering the two mechanisms of the photon emission one derives the following expression for the total amplitude of the process [14, 100, 454] (see also [414] and references therein):

$$f_{\rm tot} = f_{\rm ord} + f_{\rm pol} = \frac{4\pi(\mathbf{e}\cdot\mathbf{q})}{q^2}\left[\frac{Z_0^2}{m}\,\frac{Z-F(q)}{\omega} + Z_0\,\omega\,\alpha(\omega,q)\right], \qquad (2.1)$$

where $\mathbf{e}$ and ω are the photon polarization vector and energy, $\mathbf{q} = \mathbf{p}_1 - \mathbf{p}_2$ is the momentum transfer.

The first term in (2.1) describes the OBrS part of the amplitude. It is proportional to $Z - F(q)$, where Z is the charge of the nucleus and $F(q) = \int {\rm d}\mathbf{r}\rho(r)\exp({\rm i}\mathbf{q}\cdot\mathbf{r})$ is the form-factor of atomic electrons ($\rho(r)$ stands for an isotropic distribution of the electron charge). Hence, $f_{\rm ord}$ is dependent on the static distribution of the charge in the atom. The PBrS amplitude $f_{\rm pol}$ is expressed via a generalized atomic dynamic polarizability $\alpha(\omega, q)$ which appears as a result of the action of two field on the atom: the field of the projectile and the electromagnetic field of the emitted photon.[1]

The first feature which clearly distinguishes between the two mechanisms follows immediately from (2.1). The OBrS amplitude is inversely proportional to the mass of projectile, while the polarizational part is independent of it. The explanation for this fact follows from the basic principles of electrodynamics (see, e.g., [2]). In the OBrS process it is the projectile that emits the photon. The intensity of this radiation is proportional to the square of the projectile acceleration in the external field of a target. In turn, the acceleration is proportional to $1/m$ and this dependence appears in $f_{\rm ord}$. In contrast, during the PBrS process the projectile serves as a source of the external field acting on the atomic electrons, and thus the amplitude of this process is almost insensitive to the variations of m [414]. Moreover, the intensity of PBrS for a heavy projectile is comparable and can be even higher than that of an electron of the same velocity [33, 98].

[1] Explicit formulae for $\alpha(\omega, q)$ is presented in Sect. 2.2.1, (2.14).

Other qualitative differences between the two mechanisms of the photon emission one can trace by comparing the dependencies of $f_{\rm ord}$ and $f_{\rm pol}$ on the photon energy and on the momentum transfer.

The OBrS amplitude is a smooth function of ω. The only peculiarity appears in the soft-photon region $\omega \to 0$ where a simple perturbative approach, giving an infinite magnitude of $f_{\rm ord}$, fails to describe the process. This phenomenon, known as the "infrared catastrophe", had been recognized and understood long ago (e.g. [2]). The q dependence of $f_{\rm ord}$ is concentrated in the factor $Z - F(q)$. The atomic form-factor $F(q)$ is the Fourier image of the electron charge distribution and is a monotonically decreasing function of q. Qualitatively, the value $F(q)$ defines the number of atomic electrons inside the sphere of a radius $r \sim 1/q$. Hence, this function reaches its maximum value at $q = 0$ where $F(0) = Z$ and decreases monotonically with the increase of q. In the case of large q, $\lim_{q\to\infty} F(q) = 0$. The natural scale to measure the magnitude of q is the inverse radius of the target, $R_{\rm at}^{-1}$. Thus, the amplitude of OBrS is large for $q > R_{\rm at}^{-1}$ while in the region $q \ll R_{\rm at}^{-1}$ it becomes negligibly small. Such behaviour has a clear explanation [348]. To radiate a photon via the ordinary mechanism a projectile must penetrate inside the atom, at a distance $r < R_{\rm at}$, where a strong nuclear potential $-Z/r$ is less screened by the electron cloud. In the opposite limit, when $r \gg R_{\rm at}$, the nucleus is fully screened by the electrons (in the case of a neutral target) and the probability for a projectile to get the acceleration and to radiate vanishes.

The PBrS appears as a result of the alteration of the atomic dipole moment induced during the collision.There are two external fields—the field the photon and the Coulomb field of the projectile—which act on the atom in this process. The dynamic response of the target depends, therefore, on the parameters of both fields. Formally, it is reflected in the dependence of the generalized dynamic polarizability $\alpha(\omega, q)$ on two variables. We use the term 'generalized' when addressing to $\alpha(\omega, q)$ in order to stress the dependence on q, and, thus, to distinguish this quantity from the dipole dynamic polarizability, $\alpha_{\rm d}(\omega)$, to which $\alpha(\omega, q)$ reduces in the limit of small transferred momenta:

$$\lim_{q\to 0} \alpha(\omega, q) = \alpha(\omega)\,. \tag{2.2}$$

The dependence on q appears because of the action of the external Coulomb field of the projectile. This field distorts the electrons' orbits and induces a dipole moment of the atomic system. The dipole polarization of the electron cloud is most pronounced if the Coulomb field of the projectile is uniform on the scale of $R_{\rm at}$, i.e. when the projectile is outside the target, $r \gg R_{\rm at}$. These distances correspond to small values of the transferred momentum $q \ll R_{\rm at}^{-1}$ where, in accordance with (2.2), the PBrS amplitude, as well as the cross section, can be expressed through $\alpha_{\rm d}(\omega)$. For small distances, $r \ll R_{\rm at}$, the field of the projectile is almost spherically symmetric, so that it induces small dipole moment on the target. Hence, in contrast to the OBrS process, it is the large distances between the projectile and the target which are of the most importance for the PBrS mechanism [45, 454].

Therefore, although in the case of light projectiles (electron, positron) two mechanisms of BrS formation must be treated simultaneously, it is possible, in principle, to distinguish the photons emitted via the polarizational mechanism from those which are formed through the ordinary one. To do this it is necessary to detect the emitted photon in coincidence with the scattered particle. Then, the "polarizational" photons will be observed together with the projectile scattered at small angles (corresponding to the transferred momenta $q < R_{\rm at}^{-1}$), while large scattering angles correspond to the emission of the "ordinary" photon. This consideration is valid for neutral atoms but does not hold for ions, since in the latter case a long-range Coulomb potential leads to the emission of the photon via the ordinary mechanism for small-angle scattering of the projectile.

The dependence of $\alpha(\omega, q)$ on ω reflects the ability of the electron cloud to be dynamically polarized by an external electromagnetic field of a given frequency. In a many-electron atom, the electrons are distributed among the atomic subshells. Each subshell is characterized by an ionization potential I. In terms of classical mechanics, this corresponds to the frequency of the rotation of electrons of a given subshell around the nucleus. Using this analogy, one may say that the dynamic response of the electron cloud to the external field increases for those ω which are close to the ionization thresholds of the target subshells. Therefore, in the region

$$I_1 < \omega < I_{1s}, \tag{2.3}$$

where I_1 and I_{1s} stand, respectively, for the ionization potentials of the outermost shell and of the $1s$ shell, the function $\alpha(\omega, q)$ is non-monotonic with extrema in vicinities of the ionization potentials [6, 7, 414, 454] .

This happens, in particular, when the photon energy lies within the region of a giant dipole resonance of the photoionization cross section of a many-electron atomic subshell [8]. As far as we are aware, for the first time wide maxima in the emission spectra were observed experimentally in electron scattering from solid-state Ba, La and Ce [285, 286]. Later the theoretical explanation was given [432] which related the maxima to the virtual excitations of the $3d$-subshell electrons. In [451] a powerful maximum was observed in the emission spectrum in electron-La collision. In the subsequent paper [45] for the first time an important conclusion was drawn about the common nature of the giant resonances in photoionization and those in PBrS spectra. To reveal this similarity one recalls that at large distances between the projectile and the atom the amplitude of the PBrS process is proportional to the dipole dynamic polarizability, $\alpha_{\rm d}(\omega)$. The imaginary part of this quantity is related to the photoionization cross section $\sigma_\gamma(\omega)$ through (e.g. [81]): $\mathrm{Im}\,\alpha_{\rm d}(\omega) = c/4\pi\omega\ \sigma_\gamma(\omega)$, where $c \approx 137$ is the speed of light. Since the OBrS amplitude is real, the modulus square of the imaginary part of $f_{\rm pol}$ enters the total BrS cross section as an additive term. Therefore, a maximum in $\sigma_\gamma(\omega)$ manifests itself in the BrS spectrum as well reflecting the collective nature of the dynamic response of atomic electrons.

Although based on the assumption that main contribution to $f_{\rm pol}$ comes from the region of large distances $r \gg R_{\rm at}$, which does not always lead to a correct quantitative result, the qualitative arguments of [45] provided a clear physical explanation of the

nature of powerful maxima in emission spectra. The experiments, carried out later, supported the theoretical prediction. The maxima in the BrS spectra were measured for Ba and several rare-earth elements [382, 430, 450, 453], for La and for atoms from the lanthanum group [452], for Xe [160–163, 401, 426–428, 430] and for Ba [430] (see also the review paper [429] in [358]). In all these experiments, performed for various energies of the incoming electron (ranging from several hundreds of eV up to several keV), the powerful BrS maxima were observed for photon energies within the ranges of the giant resonances in the photoionization cross section of the $4d$ subshells.

In general, in the whole ω-region defined by (2.3), a highly non-monotonic behaviour of the generalized polarizability of a many-electron atom results in a series of peculiarities (maxima, minima, cusps) in the total BrS spectrum. The important role of the polarizational mechanism in forming the total BrS spectra in atomic collisions over a wide range of photon energies was analyzed theoretically (see the reviews [7, 9, 65, 66, 260, 261, 335, 351, 358, 414, 435] and experimentally [157–159, 161, 203, 345, 346, 356, 357, 435].

For the photon energies noticeably higher than the $1s$ ionization potential, $\omega \gg I_{1s}$ (but still in the dipole-photon domain, $\lambda \gg R_{at}$, with $\lambda = 2\pi c/\omega$ being the radiation wavelength) the atomic electrons can be effectively treated as (quasi-)free ones. Consequently, the ω dependence of $\alpha(\omega, q)$ is much like that for the cloud of free electrons. The leading term in the expansion of $\alpha(\omega, q)$ in powers of ω/I_{1s} reads [12,100]:

$$\alpha(\omega, q) \approx -\frac{F(q)}{\omega^2}\,. \tag{2.4}$$

As a result, for a fast electron ($m = 1$, $Z_0 = -1$) the total amplitude (2.1) reduces to the BrS amplitude on a bare nucleus [100]:

$$f_{\rm tot}\Big|_{\omega \gg I_{1s}} \approx \frac{4\pi(\mathbf{e}\cdot\mathbf{q})}{q^2}\,\frac{Z}{\omega}\,. \tag{2.5}$$

This shows that for large ω the atomic electrons do not participate in the screening of the nucleus and do not contribute to the BrS cross section. Thus, in the region $\omega \gg I_{1s}$ the polarizational channel results in a (dynamic) de-screening of the nucleus.

The physical reason for this effect (following [12] we use the term 'stripping' effect) is that, for $\omega \gg I_{1s}$, the electrons of all atomic subshells may be treated as free ones [100]. If the incident electron is also free (the Born approximation), then there is no dipole radiation by a system of free electrons [278].

These arguments were exploited in [12] to construct an approximate expression for the total BrS amplitude for photon energies lower than the $1s$-shell ionization threshold. To this end, the target electrons are divided into two groups, the 'inner' and the 'outer' electrons. The 'inner' electrons have binding energies $I_{\rm in} > \omega$, and, therefore, their orbits are not distorted noticeably by an external electromagnetic field of a frequency ω. As a result, the contribution of the inner electrons to the PBrS amplitude is ignored. The 'outer' electrons have binding energies $I_{\rm out}$ less than ω, so

that they behave as quasi-free particles under the action of the field, and contribute to $f_{\rm pol}$ in accordance with (2.4) where $F(q)$ must be substituted with the form-factor of the outer electrons, $F_{\rm out}(q)$. As a result the total BrS amplitude acquires the form

$$f_{\rm tot}\Big|_{I_{\rm out}<\omega<I_{\rm in}} \approx \frac{4\pi(\mathbf{e}\cdot\mathbf{q})}{q^2}\,\frac{Z-F_{\rm in}(q)}{\omega}\,, \tag{2.6}$$

where $F_{\rm in}(q)$ stands for the form-factor of the inner electrons. This expression demonstrates that the outer electrons do not participate in the screening of the nucleus (or, in other words, the nucleus is 'stripped' by a total number $N_{\rm out}$ of the outer electrons) [12]. The physical reason for this partial 'stripping' is as formulated above: for $\omega \gg I_{\rm out}$ the outer electrons are quasi-free, and, thus, no dipole radiation is emitted by the system 'projectile electron + the outer electrons'.

Although the 'stripping' approximation does not account for specific details of the PBrS amplitude in the vicinity of each threshold, it allows one to estimate the behaviour the BrS cross section below and above the threshold. In particular, the asymmetry of the giant resonances in the experimentally measured emission spectra [382, 426, 452] was explained. The experiments indicated that the magnitude of total BrS cross section far above the 4d-thresholds exceeds that below the threshold. The explanation is as follows. Equation (2.6) suggests, that the difference between the amplitude $f_{\rm tot}$ at $\omega \gg I_j$ (I_j is the ionization potential of atomic jth subshell) exceeds $f_{\rm tot}$ at $\omega \ll I_j$ by a factor proportional to $F_j(q)$. The latter can be estimates as $F_j(q) \approx N_j$, where N_j is the number of the electrons in the subshell. Therefore, the difference between the two amplitudes is proportional to N_j, and the increase in the cross section is $\sigma(\omega \gg I_j) - \sigma(\omega \ll I_j) \propto N_j^2$ [12].

This qualitative explanation was confirmed by numerical calculations [13] carried out within the framework of the non-relativistic BA. Later, the 'stripping' approximation was extended beyond the BA [73, 236, 251, 252].

In the range of photo energies below the first ionization threshold, I_1, of the target,one can expect the decrease in the contribution of the PBrS channel to the total spectrum. It follows from (2.1), that this limit $f_{\rm pol} \propto \omega\alpha(0,q) \sim \omega\alpha_{\rm d}$, where $\alpha_{\rm d}$ is a static dipole polarizability of the target. Thus, $f_{\rm pol} \to 0$ as $\omega \to 0$ in contrast to the OBrS term which behaves as $\propto 1/\omega$. Thus, the ratio $f_{\rm pol}/f_{\rm ord} \sim m\omega^2\alpha_{\rm d}/e$ vanishes as ω goes to zero. For low but non-zero values of ω the contribution of the PBrS channel strongly depends on the magnitude of the static polarizability. The higher the magnitude of $\alpha_{\rm d}$ is, the wider is the ω interval where the contribution of $f_{\rm pol}$ might be noticeable.

These arguments are valid also beyond the range of validity of the first BA, on the basis of which (2.1) was derived. In the low-frequency limit, the OBrS amplitude is expressed in terms of the elastic scattering amplitude, $f_{\rm ord} \propto f_{\rm el}/\omega$ (e.g., [81]). On the other hand, the PBrS process occurs most effectively at large distances between the projectile and the target, where the wavefunction of the projectile is not distorted strongly by the potential, so that one can extend the range of applicability of the BA for the PBrS channel even to the domain of low projectile velocities. Therefore, the ratio of the amplitudes still is proportional to $\omega^2\alpha_{\rm d}$. In [455], the

role of the polarizational channel was studied in the inverse BrS process (i.e. BrS absorption) for slow electrons scattered from atoms. It was demonstrated that for an e^-−Ar scattering the polarizational mechanism changes noticeably the absorption coefficients, whereas for an e^-−Ne scattering its influence is much less. This quantitative effect is due to large difference in the static polarizabilities: $\alpha_d^{Ar} = 11.10$ a.u. and $\alpha_d^{Ne} = 2.66$ a.u. [360]. Rather strong effect of the target polarization on the BrS spectra was reported in [142, 186–188] for low-energy ($\varepsilon_1 = 0.4 \ldots 3.5\,\mathrm{eV}$) electron–rare-gas atom collisions.

In the collisions of slow heavy particles with atoms both the OBrS and the PBrS mechanisms fail, as a rule, to describe adequately the radiation spectrum. In such processes another channel, known as molecular orbital radiation, becomes important (see, e.g., [173]). Nevertheless, the PBrS is important in asymmetric slow collisions of atoms and ions in the region of large impact parameters [388]. The intensity of the OBrS is negligibly small due the large masses of the colliders.

In the collision of a slow charged particle with an excited hydrogen atom, H^*, there appears additional and quite peculiar source of low-frequency photon emission [240]. The specific feature of the hydrogen atom introduces the linear Stark effect (see, e.g., [279]). The electric field of the projectile splits initially degenerated levels of H^*. Atomic states with a given principal number form a Stark multiplet. The components of the multiplet already possess a dipole moment. The vector of this dipole moment rotates following the movement of the projectile, and the radiation appears as a result of this rotation. We stress that this mechanism of BrS is intrinsic for systems with a linear Stark effect. This is also a distinguishing feature from the 'real' PBrS which also appears because of the alteration of the target's dipole moment. In the latter case, it is really the induced dipole moment intrinsic for systems with a quadratic Stark effect. As a result the character of these spectra at low frequencies are quite different [240].

Once the internal dynamic structure of a target is taken into account, the next logical step is to consider the radiative processes which are accompanied by the excitation or ionization of the target. Following [39, 56] we call BrS processes of this type 'inelastic' BrS contrary to the 'elastic' one, when the target does not change its state after the collision.

It is important to establish the contribution of inelastic channels to the total emission spectrum. This is not purely of theoretical interest since experimentally it is quite difficult to separate elastic and inelastic channels. To do this it is necessary to observe the final state of the target with simultaneous detection of the photon. The comparison of the contributions of the 'elastic' and 'inelastic' channels is discussed in more detail in Sects. 5.3 (non-relativistic collisions) and 6.4 (relativistic collisions). Here we only mention the main results obtained.

It has been demonstrated that over a wide region of the photon frequencies, the elastic channel dominates over the inelastic one in the total BrS spectrum for both heavy [37, 56, 98, 414] and light [36, 56, 98, 414] projectiles scattered on a many-electron atom. Semi-quantitatively, the cross sections of the elastic BrS, of both the ordinary and the polarizational nature, exceed those of the inelastic by a factor Z. The explanation is as follows [36, 37]. During the elastic BrS the contributions of

each atomic electron to the polarizational part of the total amplitude (see (2.1) are coherent, as in the process of Rayleigh scattering of light. Considering the case of a neutral atom and having in mind that the ordinary part of the elastic BrS spectrum is approximately proportional to the nuclear charge squared, one finds that the total elastic cross section is proportional to Z^2. In contrast, during the inelastic BrS the contributions of each electrons must be summed in the cross section rather than in the amplitude. Hence, the inelastic BrS cross section is proportional to Z and is parametrically small in the case of a many-electron target, when $Z \gg 1$.

The region of the photon frequencies, in which the coherence effect plays an essential role, is estimated as [36, 37, 56]

$$I_1 < \omega < \frac{v_1}{R_{\rm at}} \tag{2.7}$$

where v_1 is the initial velocity of projectile. Beyond the region of coherence inelastic BrS becomes more important. An exception of this rule occurs in collisions of fast heavy charged particles with atoms/ions collisions (as well as in atom-atom, ion-atom and ion-ion) in the region of high photon frequencies. In this region the process of inelastic BrS has a threshold, which is equal to $\omega_{\rm max} \approx v_1^2/2$. However, the elastic BrS takes place at higher energies, up to $\omega \geq 2v_1^2$, dominating in this region in the total photon emission spectrum. Therefore, the photon energy range $v_1^2/2 \leq \omega \leq 2v_1^2$ is convenient for the observation of the elastic PBrS. We note that in this ω region there is a peculiar feature in the spectrum of PBrS [241] similar to that which occurs in inelastic scattering, where it is known as the Bethe ridge [279]. In more detail we discuss this phenomenon in Sect. 4.7.

Numerical comparison of the relative role of elastic and inelastic channels in proton-atom collisions was performed in [59, 237, 241].

In electron/positron–many-electron atom scattering elastic BrS dominates parametrically over the inelastic one in the region (2.7). However, if one is interested in accurate data on the total BrS cross section it is necessary to include the inelastic channels into the computational scheme. Up to now, mostly due to technical difficulties, numerical investigations of the role of inelastic BrS have not been as extensive as in the elastic case. The achievements in this field include the model theoretical study carried out in [428, 456] in connection with the experimental data on the intensity of the BrS spectrum in e^-+Xe collision as a function of the incoming electron energy ε_1 [401, 428] (see also [157, 158] for the experimental data in non-relativistic e^-+Ar collision and the calculations made in [51] for the relativistic e^-+Ar).

For low-Z targets the absolute magnitudes of both terms from (2.1), $f^{\rm ord}$ and $f^{\rm pol}$, and the terms $f_{\rm ord}^{(m)}$ and $f_{\rm pol}^{(m)}$ from the inelastic BrS amplitude (see (5.22) in Sect. 5.3) are all of the same order. In this case, it is the charge of the projectile which introduces peculiarities in the total radiative spectrum. It can be shown that, both for high frequencies of the photon, $\omega \gg v_1/R_{\rm at}$ [37, 98] and for the low ones, $\omega \ll 1$ [37, 237] the role of inelastic channels is negligibly small compared with the elastic BrS in the case of electron scattering, while for the positron-atom collision the situation is the opposite. It occurs mainly because of the difference in the behaviour

of the interference between the ordinary and polarizational amplitudes in inelastic BrS. The interference is negative in the case of the electron projectile and positive in the positron case. The simplest way to trace this effect is to consider the inelastic BrS amplitude (5.22) in the limit of high photon frequencies, as was done above for elastic BrS. Having done this, one notices that for a projectile electron the ordinary and polarizational terms cancel each other out [37, 100, 414] while for a positron the effect is opposite [98, 414].

To conclude this section we mention theoretical approaches used to describe the BrS process in non-relativistic collisions. These can be subdivided into three parts: (a) methods applied to describe the scattering process, (b) models used for the interaction with the photon, and (c) approximations used to describe the dynamic atomic response.

The theoretical approaches to the scattering process range from the plane-wave BA to more sophisticated ones. Since the OBrS phenomenon has much longer history, these methods were first tested in application to this process and later on were applied to the PBrS problem. In application to the BrS problem in electron–atom scattering the models beyond the plane-wave BA used in both the non-relativistic and the relativistic domains include the corrections due to the Elwert factor and its modifications [70, 73, 131, 281],the use of Sommerfeld-Maue functions [81, 131, 281], the approaches based on the classical [135, 227]and semi-classical [49, 65, 234] scattering theories. The best available results have been obtained using the distorted partial-wave expansion of the projectile wavefunction. This scheme has been applied to study the ordinary BrS process of non-relativistic projectiles in the dipole-photon approximation [405, 406, 445, 446]. The most adequate description of the process has been obtained by applying the (relativistic) DPWA accompanied by the multipole series for the projectile-photon interaction operator, see, for example, the review articles [189, 327, 347, 348, 350] and research papers [133, 223, 281, 380, 381, 407–412, 443]. and references therein.

In many papers on the PBrS problem the non-relativistic Born approximation was used for both light (a positron, an electron) and heavy (a proton, an ion) projectiles. Although the range of validity of the Born approximation for PBrS is larger than for OBrS, to obtain more accurate data on the total BrS cross sections of a light projectile it is necessary to go beyond this scheme. Therefore, the non-relativistic DPWA formalism was developed [20, 27–29, 244] and applied to calculate the cross sections $\mathrm{d}\sigma$ and $\mathrm{d}^2\sigma$ over a broad spectral range [246, 248–250, 253, 257, 365] for non-relativistic electrons scattered on many-electron atoms. The partial-wave approach was also used to study the PBrS process of slow electrons [166, 273–275, 455]. To describe low-energy ($\varepsilon_1 \sim 10^0 \ldots 10^1$ eV) electron scattering from highly polarizable targets (metallic clusters, fullerenes) it is necessary to go beyond the frozen-core static potential (even supplemented with the static long-range polarizational potential $V_{\mathrm{pol}} = -\alpha_{\mathrm{d}}(0)/2r^4$). To this end, the approach was developed [113, 200] to calculate the partial wavefunctions of the scattering electron as solutions of the Dyson equation with the non-local polarization potential [19, 107, 175].

In most of the papers the dynamic atomic response to the joint actions of the field of the projectile and of the radiation field was treated within the frame of the

non-relativistic dipole-photon theory (with exception for several papers mentioned below). Even within this framework the accurate calculation of the generalized polarizability $\alpha(\omega, q)$ is not a simple task. Apart from the case of a hydrogen atom (or hydrogen-like ion) where the analytical evaluation is possible [99, 125, 257] one has to use more sophisticated approaches to calculate this quantity. The methods known to us include the HF-based calculations with the inclusion of many-body corrections, [12, 13, 20, 69, 244–248, 253], the statistical model of the atom [59–66] based on the theory of the inhomogeneous electron gas [292]. Another semi-empirical approach for effective and quite accurate calculation of $\alpha(\omega, q)$ in the vicinity of giant resonances was proposed initially for many-electron targets, [242, 243, 245], and later on was applied to fullerene and clusters [114, 115, 200, 300, 391]. The approach proposed in [256] is based on the use of the non-relativistic Coulomb Green function, and is valid for the calculation of $\alpha(\omega, q)$ in the vicinities of K- and L-shells.

Beyond the dipole-photon approximation the PBrS was considered in collisions of a non-relativistic heavy projectile with many-electron atom [38, 39, 56, 57, 168, 389]. In these papers the corrections of the order $kR_{\rm at} \ll 1$ were considered and it was demonstrated that they lead to the additional modification of the angular distribution of the radiation. More systematic analysis of the non-dipole corrections has become available recently within the framework of the full relativistic description of the PBrS process, see Chap. 5.

2.2 Non-Relativistic Distorted Partial Waves Approximation

In this section we consider the BrS emission formed in electron–atom collisions in the domain of intermediate energies ε of the incoming electron. The term 'intermediate energy' implies that the initial, ε_1, and final, ε_2, energies are, on the one hand, not too high to justify the application of the Born approximation, but on the other hand, not too low to implicate the consideration of the exchange effects between the projectile and the target electrons. An adequate description of the collision process at intermediate energies is obtained by using the distorted partial-wave approximation (DPWA) (see, for example, [330]). It is used below to construct the BrS amplitude and evaluate the partial-wave series of the cross sections [20, 29].

2.2.1 DPWA Series for BrS Amplitude

The total BrS amplitude

$$f_{\rm tot} = f_{\rm ord} + f_{\rm pol} \tag{2.8}$$

treated in the first order of the non-relativistic perturbation theory in the electron–dipole-photon interaction, can be presented by the Feynman diagrams presented in Fig. 2.2. The first diagram stands for the OBrS amplitude, $f_{\rm ord}$, while the last two describe the term $f_{\rm pol}$. The solid straight lines in the diagrams describe the initial

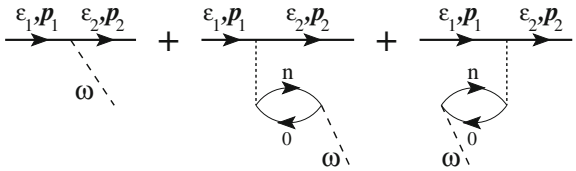

Fig. 2.2 Diagrammatic representation of the amplitude of BrS in the lowest order of the non-relativistic perturbation theory in electron–dipole-photon photon interaction. The *first diagram* describes the OBrS process, the *second* and the *third* one stand for PBrS

and the final states of the incoming particle (for clarity, we will term the projectile as 'electron') in the static field of the target atom (or ion). Other notations are as in Fig. 2.1.

As drawn, the BrS amplitude does not account for the exchange between the projectile and the target electrons. We also assume that the electron energy before, ε_1, and after, ε_2, the collision are high enough in comparison with the ionization potentials of the atomic subshells which provide the main contribution to the target polarization by the electromagnetic field of the frequency ω. The latter satisfies the strong inequality $\omega R_{\rm at}/c \ll 1$ which implies the validity of the dipole approximation, when the emission wavelength $\lambda = 2\pi c/\omega$ exceeds greatly the atomic size $R_{\rm at}$.

General analytical expressions for the terms $f_{\rm ord}$ and $f_{\rm pol}$, corresponding to the presented diagrams, are as follows:

$$f_{\rm ord} = \left\langle \mathbf{p}_2^{(-)} \left| \mathbf{e}\cdot\mathbf{r} \right| \mathbf{p}_1^{(+)} \right\rangle, \tag{2.9}$$

$$f_{\rm pol} = -\sum_n \left[\frac{\langle 0 \left| \mathbf{e}\cdot\mathbf{D} \right| n \rangle \left\langle \mathbf{p}_2^{(-)} n \left| \hat{V} \right| \mathbf{p}_1^{(+)} 0 \right\rangle}{\omega_{n0} - \omega - \mathrm{i}0} + \frac{\left\langle \mathbf{p}_2^{(-)} 0 \left| \hat{V} \right| \mathbf{p}_1^{(+)} n \right\rangle \langle n \left| \mathbf{e}\cdot\mathbf{D} \right| 0 \rangle}{\omega_{n0} + \omega} \right]. \tag{2.10}$$

Here $|\mathbf{p}_1^{(+)}\rangle$ and $|\mathbf{p}_2^{(-)}\rangle$ denote, correspondingly, the initial and the final scattering states of the electron with the asymptotic momenta $\mathbf{p}_1$ and $\mathbf{p}_2$. The '$\pm$' superscripts correspond to the outgoing ('+') and to the incoming ('−') spherical waves in the asymptotic form of the electron wavefunction. The general form of the DPWA series for these states are:

$$\left| \mathbf{p}^{(\pm)} \right\rangle = 4\pi \sqrt{\frac{\pi}{p}} \sum_{lm} \mathrm{i}^l \, \exp\left(\pm \mathrm{i}\delta_l(p)\right) \, \frac{P_\nu(r)}{r} \, Y^*_{lm}(\mathbf{n}_\mathbf{p}) Y_{lm}(\mathbf{n}_\mathbf{r}) \,. \tag{2.11}$$

Here δ_ν are the phaseshifts, the notation ν stands for a set of quantum numbers (p, l). The radial wave functions $P_\nu(r)$ satisfy the Schrödinger equation in the static potential created by the target atom in its ground state (the so-called 'frozen core' approximation). The factor in front of the sum implies that the radial wave functions are normalized to the delta function of energy measured in Rydberg. The notation

$Y_{lm}(\mathbf{n_a})$ stands for the spherical harmonics [420] dependent on the spherical angles of the unit vector $\mathbf{n_a}$ along the vector $\mathbf{a}$.

Vector $\mathbf{D}$ in (2.10) is the operator of the dipole interaction of the atomic electrons with the electromagnetic field, $\omega_{n0} = E_n - E_0$ is the energy of the atom's transition from the ground state 0 to the virtually excited state n (including excitations into the continuum).

The PBrS amplitude (2.10) can be expressed in terms of the generalized dynamic polarizability $\alpha(\omega, q)$ [244]. To facilitate this, one can make use of the Fourier transformation of the operator $\hat{V}$, which stands for the Coulomb interaction between the projectile ($\mathbf{r}$) and the atomic electrons ($\mathbf{r}_a$):

$$\hat{V} = \sum_a \frac{1}{|\mathbf{r} - \mathbf{r}_a|} = \frac{1}{2\pi^2} \sum_a \int \frac{d^3\mathbf{Q}}{Q^2} \exp(-i\mathbf{Q} \cdot (\mathbf{r} - \mathbf{r}_a)). \tag{2.12}$$

Here the sum is carried out over all electrons.

Introducing (2.12) into (2.10) one derives:

$$f_{pol} = -\frac{1}{2\pi^2} \int \frac{d^3\mathbf{Q}}{Q^2} \left\langle \mathbf{p}_2^{(-)} \left| e^{-i\mathbf{Q}\cdot\mathbf{r}} \right| \mathbf{p}_1^{(+)} \right\rangle \times \sum_n \left[\frac{\langle 0 | \mathbf{e} \cdot \mathbf{D} | n \rangle \langle n | \sum_a e^{i\mathbf{Q}\cdot\mathbf{r}_a} | 0 \rangle}{\omega_{n0} - \omega - i0} + \frac{\langle 0 | \sum_a e^{i\mathbf{Q}\cdot\mathbf{r}_a} | n \rangle \langle n | \mathbf{e} \cdot \mathbf{D} | 0 \rangle}{\omega_{n0} + \omega} \right]. \tag{2.13}$$

For a spherically symmetric target the $\sum_n [\dots]$ is related to the generalized dynamic polarizability of the atom, $\alpha(\omega, Q)$:

$$i(\mathbf{e} \cdot \mathbf{Q})\alpha(\omega, Q) = \sum_n \sum_a \left[\frac{\langle 0 | \mathbf{e} \cdot \mathbf{D} | n \rangle \langle n | e^{i\mathbf{Q}\cdot\mathbf{r}_a} | 0 \rangle}{\omega_{n0} - \omega - i0} + \frac{\langle 0 | e^{i\mathbf{Q}\cdot\mathbf{r}_a} | n \rangle \langle n | \mathbf{e} \cdot \mathbf{D} | 0 \rangle}{\omega_{n0} + \omega} \right]. \tag{2.14}$$

In the limit of small Q the polarizability $\alpha(\omega, Q)$ reduces to the dipole dynamic polarizability, $\alpha(\omega)$:

$$\lim_{Q \to 0} \alpha(\omega, Q) = \alpha(\omega) = \frac{2}{3} \sum_n \frac{\omega_{n0} \langle 0 | \mathbf{D} | n \rangle \langle n | \sum_a \mathbf{r}_a | 0 \rangle}{\omega_{n0}^2 - \omega^2 - i0}. \tag{2.15}$$

Thus, for f_{pol} one can write

$$f_{pol} = -\frac{i}{2\pi^2} \int d\mathbf{Q} \frac{\mathbf{e} \cdot \mathbf{Q}}{Q^2} \left\langle \mathbf{p}_2^{(-)} \left| e^{-i\mathbf{Q}\cdot\mathbf{r}} \right| \mathbf{p}_1^{(+)} \right\rangle \alpha(\omega, Q). \tag{2.16}$$

Expression (2.16) is obtained within the frame of the DPWA. In connection with the PBrS process was applied for the first time in [20] (see, also, [28, 29]). Expression (2.16), however, differs from the formulae for f_{pol} presented in the cited works in

that that it explicitly establishes a relationship between the amplitude of PBrS and the generalized polarizability of the target. This form of representation of $f_{\rm pol}$ has several advantages.

In many cases the dynamic response of an atom to the field of a projectile and that of a photon, which leads to the PBrS emission, bears essentially many-electron features. Therefore, its correct description implies the use of the methods developed within the framework of many-body perturbation theory. The fact, that $f_{\rm pol}$ can be expressed only via $\alpha(\omega, Q)$, which contains all the necessary information on the atomic dynamic response, can simplify theoretical and numerical analysis of the PBrS process (see, Chap. 4 for the examples).

The representation of $f_{\rm pol}$ in the form (2.16) allows one to easily carry out the Born limit of the PBrS amplitude. For doing this, one substituting the distorted waves $\left|\mathbf{p}_{1,2}^{(\pm)}\right\rangle$ with the wavefunctions of a free movement, $\left|\tilde{\mathbf{p}}_{1,2}^{(\pm)}\right\rangle = \exp(\mathrm{i}\mathbf{p}_{1,2}\cdot\mathbf{r})$, and accounting for the relation

$$\langle\tilde{\mathbf{p}}_2^{(-)}\,|\exp(-\mathrm{i}\mathbf{Q}\cdot\mathbf{r})|\,\tilde{\mathbf{p}}_1^{(+)}\rangle = (2\pi)^3\delta(\mathbf{q}-\mathbf{Q}),$$

one obtains an expression for $f_{\rm pol}$ within the frame of the plane-wave Born approximation (cf. (2.1)):

$$f_{\rm pol}^{\rm B} = -4\pi\mathrm{i}\frac{\mathbf{e}\cdot\mathbf{q}}{q^2}\,\alpha(\omega, q). \tag{2.17}$$

This expression for the PBrS amplitude as well as the corresponding formulae for the spectral and angular distribution of the radiation were presented for the first time in [14].

Using (2.11) in (2.9) and (2.16) one obtains, after some angular algebra, the expansion of $f_{\rm ord}$ and $f_{\rm pol}$ in partial series. The structure of both series is similar and is given by the following general expression:

$$f = \frac{16\pi^3}{\sqrt{p_1 p_2}}\sqrt{\frac{4\pi}{3}}\sum_{l_1 l_2}\mathrm{i}^{l_1-l_2}\mathrm{e}^{\mathrm{i}\left(\delta_{l_1}(p_1)+\delta_{l_2}(p_2)\right)}(-1)^{l_>}\sqrt{l_>}\,T_{l_2 l_1}\left(\mathbf{n}_\mathbf{e}, \mathbf{n}_{\mathbf{p}_1}, \mathbf{n}_{\mathbf{p}_2}\right)R_{l_2 l_1}. \tag{2.18}$$

Here $l_2 = l_1 \pm 1$ in accordance with the dipole selection rules, $l_> = \max\{l_1, l_2\}$. The factor $T_{l_2 l_1}\left(\mathbf{n}_\mathbf{e}, \mathbf{n}_{\mathbf{p}_1}, \mathbf{n}_{\mathbf{p}_2}\right)$, dependent on the angular variables of the vectors $\mathbf{e}$, $\mathbf{p}_1$ and $\mathbf{p}_2$, is equal to

$$T_{l_2 l_1}\left(\mathbf{n}_\mathbf{e}, \mathbf{n}_{\mathbf{p}_1}, \mathbf{n}_{\mathbf{p}_2}\right) = \sum_{\substack{m_1 m_2\\ m}}(-1)^{m_2}\begin{pmatrix} l_2 & 1 & l_1\\ -m_2 & m & m_1\end{pmatrix}Y_{1m}^*(\mathbf{n}_\mathbf{e})Y_{l_1 m_1}^*(\mathbf{n}_{\mathbf{p}_1})Y_{l_2 m_2}(\mathbf{n}_{\mathbf{p}_2}). \tag{2.19}$$

Here $\begin{pmatrix} l_2 & 1 & l_1\\ -m_2 & m & m_1\end{pmatrix}$ is the 3j-symbol [420].

In (2.18) the notation $R_{l_2 l_1}$ stands for

$$R_{l_2 l_1} = \begin{cases} +R^{\rm ord}_{l_2 l_1} & \text{for OBrS} \\ -R^{\rm pol}_{l_2 l_1} & \text{for PBrS.} \end{cases}$$

The partial amplitudes of the ordinary and the polarizational BrS are expressed via the following integrals:

$$R^{\rm ord}_{l_2 l_1} = \langle \nu_2 \| r \| \nu_1 \rangle = \int_0^\infty {\rm d}r \; P_{\nu_2}(r)\, r \, P_{\nu_1}(r) \tag{2.20}$$

$$R^{\rm pol}_{l_2 l_1} = \frac{2}{\pi} \int_0^\infty {\rm d}Q \; Q \, \langle \nu_2 \| j_1(Qr) \| \nu_1 \rangle \, \alpha(\omega, Q). \tag{2.21}$$

where $j_1(Qr)$ is the spherical Bessel function [1].

The ordinary BrS emission is formed mainly at the distances ρ lower and equal, in order of magnitude, to the atomic radius, $\rho \lesssim R_{\rm at}$ (see, for example, [81, 350]. In contrast, in the PBrS process the large distances $\rho \sim p_1/\omega$ play the most important role [45, 455]. Thus, the specific angular momenta in the ordinary BrS process are $l_{\rm ord} \sim p_1 R_{\rm at}$, while for the polarizational BrS, $l_{\rm pol} \sim p_1^2/\omega$. It follows then that for sufficiently high projectile velocities $l_{\rm pol} \gg l_{\rm ord} > 1$. From the computational viewpoint this inequality means that the sum over l_1 and l_2 in (2.18) in the case of PBrS converges rather slowly, and one has to calculate a large number of partial terms to obtain an accurate result for $f_{\rm pol}$.

To avoid the technical difficulty related to slow convergence of the partial series in $f_{\rm pol}$ one can take advantage of the fact that the projectile's radial wavefunctions of large orbital momenta are weakly distorted by the static atomic potential and, thus, are close to those of a free movement. Hence, it is possible to re-write the expression for $f_{\rm pol}$, explicitly extracting the Born amplitude (2.17) from (2.18). Then, the remainder, $\Delta f_{\rm pol} = f_{\rm pol} - f^{\rm B}_{\rm pol}$ will be represented by a rapidly convergent partial series [244].

Having done this one obtains the following representation of $f_{\rm pol}$:

$$f_{\rm pol} = f^{\rm B}_{\rm pol} + \Delta f_{\rm pol} \tag{2.22}$$

The structure of the term $\Delta f_{\rm pol}$ is given by the general expression (2.18) where the partial amplitudes $R_{l_2 l_1}$ are substituted with

$$\Delta R^{pol}_{l_2 l_1} = R^{\rm pol}_{l_2 l_1} - {\rm e}^{-i\left(\delta_{l_1}(p_1) - \delta_{l_2}(p_2)\right)} \, \tilde{R}^{\rm pol}_{l_2 l_1} \, . \tag{2.23}$$

The notation $\tilde{R}^{\rm pol}_{l_2 l_1}$ is used for the integral

$$\tilde{R}^{\rm pol}_{l_2 l_1} = \frac{2}{\pi} \int_0^\infty {\rm d}Q \; Q \, \langle \tilde{\nu}_2 \| j_1(Qr) \| \tilde{\nu}_1 \rangle \, \alpha(\omega, Q) \tag{2.24}$$

The matrix element in the integrand in (2.24) is calculated between the radial wave functions of a free particle: $\|\tilde{\nu}\rangle = (p/\pi)^{1/2} r j_l(pr)$.

2.2.2 BrS Cross Section

The two-fold differential BrS cross section, which characterizes the spectral and the angular distributions of radiation, is given by

$$\frac{\mathrm{d}^2\sigma}{\mathrm{d}\omega \mathrm{d}\Omega_{\mathbf{k}}} = \frac{1}{(2\pi)^4}\frac{\omega^3}{c^3}\frac{p_2}{p_1}\int \mathrm{d}\Omega_{\mathbf{p}_2} \sum_{\lambda} |f_{\mathrm{tot}}|^2 \tag{2.25}$$

Here $\mathrm{d}\Omega_{\mathbf{k}}$ is the element of the solid angle of the emission along the vector $\mathbf{k}$ which is the photon momentum. The integral is carried out over the solid angle, $\mathrm{d}\Omega_{\mathbf{p}_2}$, of the scattered electron. The sum is taken over the photon polarizations, λ. For arbitrary vectors $\mathbf{a}$ and $\mathbf{b}$ the following general formula can be applied (see, e.q., [81]):

$$\sum_{\lambda} (\mathbf{e}_\lambda \cdot \mathbf{a})(\mathbf{e}_\lambda \cdot \mathbf{b}) = \mathbf{a}\cdot\mathbf{b} - \frac{(\mathbf{a}\cdot\mathbf{k})(\mathbf{b}\cdot\mathbf{k})}{k^2}\,. \tag{2.26}$$

The cross section (2.25) defines the probability of the photon emission within the energy interval $[\omega, \omega + \mathrm{d}\omega]$ in the solid angle $\mathrm{d}\Omega_{\mathbf{k}}$, normalized to the flux of the incident electrons.

Integrating (2.25) over the emission angles one defines the spectral distribution of BrS, which is characterized by the differential cross section:

$$\frac{\mathrm{d}\sigma}{\mathrm{d}\omega} = \int \mathrm{d}\Omega_{\mathbf{k}} \frac{\mathrm{d}^2\sigma}{\mathrm{d}\omega \mathrm{d}\Omega_{\mathbf{k}}}\,. \tag{2.27}$$

In the dipole approximation, the double differential cross section $\mathrm{d}^2\sigma/\mathrm{d}\omega\mathrm{d}\Omega_{\mathbf{k}}$ has a quite simple dependence on the emission angle $\theta_{\mathbf{k}} = \widehat{\mathbf{k}, \mathbf{p}_1}$ [69]:

$$\frac{\mathrm{d}^2\sigma}{\mathrm{d}\omega \mathrm{d}\Omega_{\mathbf{k}}} = \frac{1}{4\pi}\frac{\mathrm{d}\sigma}{\mathrm{d}\omega}\Big(1 - \beta(\omega)\, P_2(\cos\theta_{\mathbf{k}})\Big)\,. \tag{2.28}$$

$P_2(y) = (3y^2 - 1)/2$ is the Legendre polynomial of the second order. In analogy with the photoionization process, the quantity $\beta(\omega)$, which defines the profile of the angular distribution of the dipole radiation, is called angular anisotropy parameter [121].

Using (2.18)–(2.21) to construct the total BrS amplitude (2.8), and then substituting the result into (2.25) one obtains the following partial series for the cross section $\mathrm{d}\sigma/\mathrm{d}\omega$ and for the angular anisotropy parameter [29, 244]:

$$\frac{\mathrm{d}\sigma}{\mathrm{d}\omega} = \frac{32\pi^2}{3p_1^2}\frac{\omega^3}{c^3}\sum_{l=0}^{\infty}\sum_{l'=l\pm1} l_> \left|R^{\mathrm{tot}}_{l'l}\right|^2 = \frac{\mathrm{d}\sigma_{\mathrm{ord}}}{\mathrm{d}\omega} + \frac{\mathrm{d}\sigma_{\mathrm{pol}}}{\mathrm{d}\omega} + \frac{\mathrm{d}\sigma_{\mathrm{int}}}{\mathrm{d}\omega}\,. \tag{2.29}$$

$$\beta(\omega) = \left(\frac{\mathrm{d}\sigma}{\mathrm{d}\omega}\right)^{-1}\frac{16\pi^2}{3p_1^2}\frac{\omega^3}{c^3} \times \sum_l (l+1)\left\{ l\sum_{l'=l\pm1}\frac{\left|R^{\mathrm{tot}}_{l'l}\right|^2}{2l'+1} - 6\frac{l+2}{2l+3}\mathrm{Re}\left[\mathrm{e}^{\mathrm{i}\Delta_l}\, R^{\mathrm{tot}}_{l+1l}\left(R^{\mathrm{tot}}_{l+1l+2}\right)^*\right]\right\}, \tag{2.30}$$

where the following short-hand notations are used:

$$R^{\mathrm{tot}}_{l'l} = R^{\mathrm{ord}}_{l'l} - R^{\mathrm{pol}}_{l'l}\,, \qquad \Delta_l = \delta_l(p_1) - \delta_{l+2}(p_1)\,.$$

If one neglects the partial PBrS amplitude $R^{\mathrm{pol}}_{l_2l_1}$ on the right-hand sides of (2.29) and (2.30), the resulting formula coincides with the known partial-wave expansion for OBrS [385, 405, 406, 446].

Presentation of the cross section as a sum of three terms, $\mathrm{d}\sigma_{\mathrm{ord}}$, $\mathrm{d}\sigma_{\mathrm{pol}}$ and $\mathrm{d}\sigma_{\mathrm{int}}$ (2.30), although being somewhat conditional, is convenient for further analysis.

In principle, it is experimentally possible to distinguish the photons emitted via the polarization mechanism from those generated in the OBrS process.

As has been already mentioned, the domains of the impact parameters in which one of the two BrS mechanisms dominates are well separated provided the condition $p_1/\omega \gg R_{\mathrm{at}}$ is fulfilled. Small impact parameters $\rho < R_{\mathrm{at}}$, which are important for OBrS, correspond to large momentum transfer, $q \sim \rho^{-1}$, or, which is equivalent, to (comparatively) large scattering angles. The polarization mechanism is of less importance, since the induced dipole moment is small. Formally, the latter statement follows from the definition of the generalized polarizability, (2.14). Indeed, for large values transferred momenta, $Q \gg 1/R_{\mathrm{at}}$ the exponent $\exp(\mathrm{i}\mathbf{Q}\cdot\mathbf{r}_a)$ rapidly oscillates in the matrix element, resulting in $\alpha(\omega, Q) \to 0$.

As the distance between the projectile and the target becomes larger than the atomic radius, the Coulomb field of the nucleus is fully screened by the electron cloud, and the OBrS radiation is suppressed. On the contrary, the contribution of PBrS for $\rho \gg R_{\mathrm{at}}$ is enhanced since the field of the projectile is nearly uniform on the scale of R_{at}, so that the polarization of the target occurs more effectively. Large distances correspond to small transferred momenta, $q \ll R_{\mathrm{at}}$ and, correspondingly, to small scattering angles.

Therefore, to distinguish between the polarizational and ordinary BrS, the experimental setup should allow one to detect the photon and the scattered electron simultaneously. Then the PBrS will be predominantly detected for small-angle scattering events, while the large-angle scattering will give rise to the photon yield through the OBrS channel.

The arguments presented above are valid for neutral atoms. For ionic targets, the long-range Coulomb field of the net charge of the ion increases the intensity of OBrS in the domain of small-angle scattering.

For the sake of completeness and for further reference let us present the formulae for $\mathrm{d}\sigma/\mathrm{d}\omega$ and $\mathrm{d}^2\sigma/\mathrm{d}\omega\mathrm{d}\Omega_{\mathbf{k}}$ written within the framework of the plane-wave Born approximation. The formulae can be obtained directly, by using the BrS amplitude (2.1) in (2.25), or as the Born limit of (2.29) and (2.30) [29]. The result can be written as follows (see also [13]):

$$\frac{\mathrm{d}^2\sigma_{\mathrm{B}}}{\mathrm{d}\omega\mathrm{d}\Omega_{\mathbf{k}}} = \frac{1}{4\pi}\frac{\mathrm{d}\sigma_{\mathrm{B}}}{\mathrm{d}\omega}\Big[1 - \beta_{\mathrm{B}}(\omega)\,P_2(\cos\theta_{\mathbf{k}})\Big), \tag{2.31}$$

$$\frac{\mathrm{d}\sigma_{\mathrm{B}}}{\mathrm{d}\omega} = C\int\limits_{q_{\min}}^{q_{\max}}\frac{\mathrm{d}q}{q}\left|\frac{Z_0}{M}\Big(Z - F(q)\Big) + \omega^2\alpha(\omega,q)\right|^2, \tag{2.32}$$

$$\beta_{\mathrm{B}}(\omega) = \left(\frac{\mathrm{d}\sigma_{\mathrm{B}}}{\mathrm{d}\omega}\right)^{-1} C\int\limits_{q_{\min}}^{q_{\max}}\frac{\mathrm{d}q}{q}\left|\frac{Z_0}{M}\Big(Z - F(q)\Big) + \omega^2\alpha(\omega,q)\right|^2 P_2(\cos\theta_{\mathbf{q}}). \tag{2.33}$$

Here $C = 16Z_0^2/3c^3p_1^2\omega$, $q_{\min}^{\max} = p_1 \pm p_2 = p_1(1 \pm \sqrt{1-\omega/\varepsilon_1})$ are the maximum and minimum values of the transferred momentum $q = |\mathbf{p}_1 - \mathbf{p}_2|$, $\theta_{\mathbf{q}} = \mathbf{p}_1\cdot\mathbf{q}/p_1q = (q_{\max}q_{\min} + q^2)/2p_1q$.

2.3 Multipole Series for PBrS Cross Section

Let us analyze the role of quadrupole terms, as well as the higher multipoles, in the cross section of PBrS [389]. To simplify the consideration we will treat the PBrS within the BA. In Sect. 4.1 it will be demonstrated that the range of applicability of BA for the PBrS process for an electron is much broader than that for the OBrS process. As for the heavy projectiles, the BA can be applied to describe PBrS in comparatively slow collisions as well [388].

For a heavy projectile, the PBrS cross section differential in ω, the solid angle of emission and in the transferred momentum q, can be written in the form [389][2]:

$$\frac{\mathrm{d}^3\sigma_{\mathrm{pol}}}{\mathrm{d}\omega\mathrm{d}\Omega_{\mathbf{k}}\mathrm{d}q} = \frac{2Z_0^2\omega^3}{\pi c^3v_1^2q}\sum_{N=0}^{\infty}k^N\mathscr{A}_N(\omega,q)\,C_N(\cos\theta_{\mathbf{k}},\cos\theta_{\mathbf{q}}). \tag{2.34}$$

Here $\cos\theta_{\mathbf{q}} = \omega/v_1q + q/2p_1$, and the following notation is introduced:

[2] The formulae presented in this section can be also derived as a non-relativistic limit of general relativistic formalism for PBrS described in detail in Sects. 6.5.1 and 6.5.3.

$$\mathscr{A}_N(\omega, q) = \sum_{j=0}^{N} \alpha_j(\omega, q)\alpha^*_{N-j}(\omega, q). \tag{2.35}$$

For atomic targets with filled (or semi-filled) subshells, the expression for a multipole generalized polarizability $\alpha_j(\omega, q)$ (with $j \geq 1$)[3] reads

$$\alpha_j(\omega, q) = -4\mathrm{i} \sum_{n'l'} \sum_{l_1 l_2} \frac{\mathrm{i}^{l_1}(-1)^{l+l'} \mathscr{C}_{l\, j\, l_2 l_1\, l'}}{\omega_{n0}^2 - \omega^2 - \mathrm{i}0} \langle nl \| j_{l_1}(qr) \| n'l' \rangle \langle n'l' \| r^j \frac{\mathrm{d}}{\mathrm{d}r} \| nl \rangle. \tag{2.36}$$

Here n and l stand for the principal and orbital quantum numbers. The summations in (2.36) are carried out subject to the following conditions: (1) the integers l_2 and j are of the same parity and $l_2 \leq j$, (2) $l_1 = l_2 \pm 1$, (3) the integers l' and $l + l_1$ are of the same parity and $l + l_1 \geq l' \geq |l - l_1|$. The coefficient $\mathscr{C}_{l\, j\, l_2 l_1\, l'}$ is as follows:

$$\mathscr{C}_{l\, j\, l_2 l_1\, l'} = \frac{j!(2l+1)(2l'+1)(2l_1+1)(2l_2+1)}{(j-l_2)!!(j+l_2+1)!!} \begin{pmatrix} l & l_1 & l' \\ 0 & 0 & 0 \end{pmatrix} \begin{pmatrix} l_2 & 1 & l_1 \\ 0 & 0 & 0 \end{pmatrix}. \tag{2.37}$$

The coefficients C_N from (2.37) are expressed in terms of the Legendre polynomials as follows:

$$C_N(\cos\theta_k, \cos\theta_{\mathbf{q}}) = \sum_{L \leq N+2} K_{NL}\, P_L(\cos\theta_q) P_L(\cos\theta_{\mathbf{k}}), \tag{2.38}$$

where

$$K_{NL} = \frac{(2L+1)N!}{(N-L)!!(N+L+1)!!} \quad \text{for} \quad L \leq N\,.$$
$$K_{NN+2} = -\frac{N+2}{(2N+3)!!} \quad \text{for} \quad L = N+2.$$

In (2.38), parities of the summation index L and the integer N coincide.

Integrating (2.34) over the emission angle one arrives at

$$\frac{\mathrm{d}^2\sigma_{\mathrm{pol}}}{\mathrm{d}\omega \mathrm{d}q} = \frac{8Z_0^2\omega^3}{c^3 v_1^2 q} \sum_{N=0}^{\infty} \frac{k(2N)(2N)!}{(2N)!!(2N+1)!!} \left(1 - \frac{2N+1}{2N+3}\right) \mathscr{A}_{2N}(\omega, q). \tag{2.39}$$

This expression shows, that there is no interference of the photons of different multipolarity in the spectral distribution of the emitted radiation. The interference takes place in the spectral-angular distribution but vanishes in the cross section integrated over the emission angle.

[3] For $j = 0$ the term $\alpha_0(\omega, q)$ coincides with $\alpha(\omega, q)$ defined in (2.14).

The above-written formulae are simplified in the dipole-photon limit supplemented with the quadrupole correction. Thus, the dipole part of the double differential cross section (2.39) is as follows:

$$\left.\frac{\mathrm{d}^2\sigma_{\mathrm{pol}}}{\mathrm{d}\omega \mathrm{d}q}\right|_{\mathrm{dip}} = \frac{16Z_0^2\omega^3}{3c^3v_1^2q}|\alpha(\omega,q)|^2. \tag{2.40}$$

The quadrupole correction to (2.40) reads:

$$\left.\frac{\mathrm{d}\sigma}{\mathrm{d}\omega \mathrm{d}q}\right|_{\mathrm{quad}} = \frac{16Z_0^2\omega^5}{15c^5v_1^2q}\mathscr{A}_2(\omega,q), \tag{2.41}$$

where

$$\mathscr{A}_2(\omega,q) = 2\mathrm{Re}\,\alpha_0(\omega,q)\alpha_2^*(\omega,q) + |\alpha_1(\omega,q)|^2.$$

The parameter of the multipole series (2.35), (2.39) is $(\omega R_{\mathrm{at}}/c)^2$. For the photon energies comparable to the K-ionization potential of an atom with $Z \sim 10$, this parameter can be estimated as ~0.1–0.2. Hence, the quadrupole term (2.3) can provide additional 10–20 % to the yield of PBrS. The quadrupole contribution increases with Z leading to a noticeable asymmetry in the angular distribution of emitted radiation with respect to the direction $\theta_{\mathbf{k}} = \pi/2$. This effect explains some discrepancy between the experimental data [205] and the results followed from the theory of dipole PBrS.

2.4 BrS Spectrum in the Tip Region

Let us estimate the relative contributions of PBrS near the high-frequency edge [27]:

$$\varepsilon_1, \omega \gg \varepsilon_2\,. \tag{2.42}$$

Thus, it is assumed that the incident electron releases nearly all of its energy via the radiative mechanisms. The target atom is supposed to be in its ground state before and after the collision.

To evaluate the amplitudes f_{ord} and f_{pol} we adopt the Born approximation for the incoming electron, $|\mathbf{p}_1\rangle = \exp(\mathrm{i}\mathbf{p}_1 \cdot \mathbf{r})$, and consider the operator of electron–dipole-photon interaction in the form of 'velocity', $\hat{V}_\gamma = \mathbf{e} \cdot \hat{\mathbf{p}}$, rather in the form of 'length' which was used in Sect. 2.2.1 (see, for example, [385]). Then, instead of (2.9) and (2.16), one derives:

$$f_{\rm ord} = \left\langle \mathbf{p}_2^{(-)} \left| \mathbf{e}\cdot\hat{\mathbf{p}} \right| \mathbf{p}_1^{(+)} \right\rangle = (\mathbf{e}\cdot\mathbf{p}_1)\,\phi^*_{\mathbf{p}_2}(\mathbf{p}_1) \tag{2.43}$$

$$f_{\rm pol} = -\frac{\omega}{2\pi^2}\int \frac{\mathrm{d}\mathbf{q}}{q^2}\,(\mathbf{e}\cdot\mathbf{q})\,\phi^*_{\mathbf{p}_2}(\mathbf{p}_1-\mathbf{q})\,\alpha(\omega,q)\,. \tag{2.44}$$

Here $\phi_{\mathbf{p}_2}(\mathbf{Q})$ is the Fourier transform of the slow-electron wavefunction $\psi_{\mathbf{p}_2}(\mathbf{r})$:

$$\phi_{\mathbf{p}_2}(\mathbf{Q}) = \int \mathrm{d}\mathbf{r}\,\psi_{\mathbf{p}_2}(\mathbf{r})\,\mathrm{e}^{-\mathrm{i}\mathbf{Q}\cdot\mathbf{q}}\,. \tag{2.45}$$

Let us estimate the amplitudes $f_{\rm ord}$ and $f_{\rm pol}$. In the final state the electron is slow. Therefore, in the partial-wave expansion (2.11) of its wavefunction one can retain only the s-wave.[4] Then one finds

$$\phi_{\mathbf{p}_2}(\mathbf{p}_1) = -\frac{8\pi F(p_1)}{p_1^4}\,\frac{\sin\delta_s(p_2)}{p_2}\,. \tag{2.46}$$

Here $F(p_1)$ is the atomic form-factor and $\delta_s(p_2)$ is the s-wave scattering phaseshift. Introducing the scattering length $L = -\sin\delta_s(p_2)/p_2$, one obtains for the OBrS amplitude:

$$f_{\rm ord} = (\mathbf{e}\cdot\mathbf{p}_1)\,\frac{8\pi F(p_1)}{p_1^4}\,L\,. \tag{2.47}$$

To evaluate the integral in (2.44) it is necessary to examine two q-regions:

$$\text{(A)}\quad R_{\rm at}^{-1} < q \ll p_1, \qquad \text{(B)}\quad |\mathbf{p}_1-\mathbf{q}| \le R_{\rm at}^{-1}, \tag{2.48}$$

so that $f_{\rm pol} = f_{\rm pol}^{\rm A} + f_{\rm pol}^{\rm B}$. Here $R_{\rm at}$ stands for the (average) atomic radius.

In region (A) the factor $\phi^*_{\mathbf{p}_2}(\mathbf{p}_1-\mathbf{q})$ can be estimated as follows:

$$\phi^*_{\mathbf{p}_2}(\mathbf{p}_1-\mathbf{q}) \approx \phi^*_{\mathbf{p}_2}(\mathbf{p}_1) - \mathbf{q}\cdot\frac{\partial\phi^*_{\mathbf{p}_2}(\mathbf{p}_1)}{\partial\mathbf{p}_1} \sim \phi^*_{\mathbf{p}_2}(\mathbf{p}_1)\left(1-\frac{4(\mathbf{q}\cdot\mathbf{p}_1)}{p_1^2}\right). \tag{2.49}$$

This leads to

$$f_{\rm pol}^{\rm A} \approx -\frac{8\omega}{3\pi p_1^2}\,f_{\rm ord}\int_{q<R_{\rm at}^{-1}} \mathrm{d}q\,q^2\,\alpha(\omega,q) \approx -\frac{4}{9\pi R_{\rm at}^2}\,f_{\rm ord}\,\alpha(\omega)\,. \tag{2.50}$$

In the last relation in (2.50) it is taken into account that $p_1^2/2 \approx \omega$ and $\alpha(\omega,q) \approx \alpha(\omega)$ for $q \ll R_{\rm at}^{-1}$ (see (2.4)).

[4] We do not consider the case of resonant scattering in the final state with higher orbital momentum [432].

In region (B) only large distances $r > R_{\rm at}$ contribute significantly to the Fourier transform $\phi_{\mathbf{p}_2}(\mathbf{p}_1 - \mathbf{q})$ as far as $p_2 \to 0$. Then

$$\phi_{\mathbf{p}_2}(\mathbf{p}_1 - \mathbf{q}) \approx (2\pi)^3\, \delta(\mathbf{p}_1 - \mathbf{p}_2 - \mathbf{q}) - \frac{4\pi L}{(\mathbf{p}_1 - \mathbf{q})^2 - p_2^2} \tag{2.51}$$

Substituting (2.51) into $f_{\rm pol}^{\rm B}$ one obtains the following estimate:

$$f_{\rm pol}^{\rm B} \approx -f_{\rm ord}\, \frac{\omega^2 \alpha(\omega, p_1)}{F(p_1) L} \left(1 - \beta\, \frac{L}{R_{\rm at}}\right). \tag{2.52}$$

Here β is the factor of the order of 1.

Now we may estimate the ratio η of the PBrS-to-OBrS amplitudes:

$$\eta = \frac{f_{\rm pol}}{f_{\rm ord}} \sim -\frac{4}{9\pi R_{\rm at}^2}\, \alpha(\omega) - \frac{\omega^2 \alpha(\omega, p_1)}{F(p_1) L} \left(1 - \beta\, \frac{L}{R_{\rm at}}\right). \tag{2.53}$$

Despite the approximations made, one can deduce, basing on (2.53), for which energies $\varepsilon_1 \approx \omega$ the PBrS dominates in the tip region.

The quantities $\alpha(\omega)$ and $\alpha(\omega, p_1)$ have real and imaginary parts, and so does the ratio η. One can expect, that the inequality $|\eta| \gg 1$ might be met for photon frequencies at which $\mathrm{Im}\,\alpha(\omega)$ attains its maximum values. The latter are connected with the maxima of the photoionization cross section $\sigma_\gamma(\omega)$ since $\mathrm{Im}\,\alpha(\omega) = (c/4\pi\omega)\alpha(\omega)$.

The OBrS cross section in the tip region tends to zero as $(\varepsilon_1 - \omega)^{1/2}$ [81]. Hence, for the incident energies ε_1 close to the maxima of $\sigma_\gamma(\omega)$, the total BrS cross will also have maxima which are due to the PBrS channel.

Let us estimate numerically the magnitude of η for Xe [27]. The cross section $\sigma_\gamma(\omega)$ for Xe has a wide maximum above the threshold for the $4d$-subshell ($I_{4d} = 5.6$ Ryd ≈ 76 eV). At the maximum which is located at $\omega_{\max} = 7.5$ Ryd, $\sigma_\gamma(\omega)$ attains the value $\approx$30 Mb [183]. The maximum width is approximately 3 Ryd, i.e. $\omega = 6\ldots9$ Ryd, and for the estimate of η we choose ε_1 from this energy region. Let $E_1 = 7.5$ Ryd. The atomic radius in this case is the radius of the 4d-subshell: $R_{4d} \sim (2I_{4d})^{-1/2} \approx 0.4$ a.u. The imaginary part of the dipole dynamical polarizability of the 4d-subshell is $\mathrm{Im}\,\alpha(\omega_{\max}) = (c/4\pi\omega_{\max})\alpha(\omega_{\max})$; the scattering length for Xe is $L = -5.4$ a.u. Substituting these data into (2.53), one obtains $\eta = -4.5$.

This estimate demonstrates that for electron energies close to the maxima of $\sigma_\gamma(\omega)$ the polarizational part of the BrS amplitude can greatly exceed the ordinary one in the tip region of the spectrum.

http://www.springer.com/978-3-642-45223-9

Polarization Bremsstrahlung

Korol, A.V.; Solov'yov, A.V.

2014, XI, 275 p. 71 illus., 33 illus. in color., Hardcover
ISBN: 978-3-642-45223-9